

TWO-PARTICLE CONTRIBUTIONS AND NONLOCAL EFFECTS IN THE QCD SUM RULES FOR THE AXIALVECTOR TETRAQUARK CANDIDATE $Z_c(3900)$

Zhi-Gang Wang¹

Department of Physics, North China Electric Power University, Baoding 071003, P. R. China

Abstract

In this article, we study the $Z_c(3900)$ with the QCD sum rules in details by including the two-particle scattering state contributions and nonlocal effects between the diquark and antidiquark constituents. The two-particle scattering state contributions cannot saturate the QCD sum rules at the hadron side, the contribution of the $Z_c(3900)$ plays an un-substitutable role, we can saturate the QCD sum rules with or without the two-particle scattering state contributions. If there exists a barrier or spatial separation between the diquark and antidiquark constituents, the Feynman diagrams can be divided into the factorizable and nonfactorizable diagrams. The factorizable diagrams consist of two colored clusters and lead to a stable tetraquark state. The nonfactorizable Feynman diagrams correspond to the tunnelling effects, which play a minor important role in the QCD sum rules, and are consistent with the small width of the $Z_c(3900)$. It is feasible to apply the QCD sum rules to study the tetraquark states, which begin to receive contributions at the order $\mathcal{O}(\alpha_s^0)$, not at the order $\mathcal{O}(\alpha_s^2)$.

PACS number: 12.39.Mk, 12.38.Lg

Key words: Tetraquark state, QCD sum rules

1 Introduction

In 2013, the BESIII collaboration observed the $Z_c(3900)$ in the $\pi^\pm J/\psi$ mass spectrum with a mass of $(3899.0 \pm 3.6 \pm 4.9)$ MeV and a width of $(46 \pm 10 \pm 20)$ MeV, respectively [1]. The $Z_c(3900)$ was also observed by the Belle collaboration [2] and was confirmed by the CLEO collaboration [3]. The average values of the mass and width of the $Z_c(3900)$ listed in the Review of Particle Physics are $M = (3887.2 \pm 2.3)$ MeV and $\Gamma = (28.2 \pm 2.6)$ MeV, respectively [4]. There have been several possible assignments for the $Z_c(3900)$, such as tetraquark state [5, 6, 7, 8], molecular state [9, 10], hadro-charmonium [11], rescattering effect [12].

In 2014, the LHCb collaboration confirmed the $Z_c^-(4430)$ state in the $B^0 \rightarrow \psi' \pi^- K^+$ decays and established its spin-parity $J^P = 1^+$, the measured mass and width are $M = (4475 \pm 7_{-25}^{+15})$ MeV and $\Gamma = (172 \pm 13_{-34}^{+37})$ MeV, respectively [13]. In 2017, the BESIII collaboration determined the spin and parity of the $Z_c(3900)$ state $J^P = 1^+$ [14].

The $Z_c(3900)$ and $Z_c(4430)$ can be assigned to be the ground state and the first radial excitation of the axialvector tetraquark states respectively according to the analogous decays, $Z_c(3900)^\pm \rightarrow J/\psi \pi^\pm$, $Z_c(4430)^\pm \rightarrow \psi' \pi^\pm$, and the mass gaps $M_{Z_c(4430)} - M_{Z_c(3900)} = 588$ MeV $= m_{\psi'} - m_{J/\psi} = 589$ MeV [15, 16, 17, 18].

In Ref.[7], we study the axialvector hidden-charm tetraquark states with the QCD sum rules, and explore the energy scale dependence of the QCD sum rules for the tetraquark states in details for the first time. The calculations support assigning the $X(3872)$ and $Z_c(3900)$ to be the $J^{PC} = 1^{++}$ and 1^{+-} diquark-antidiquark type tetraquark states, respectively. In Refs.[8, 19, 20], the two-body strong decays of the $Z_c(3900)$ are studied with the QCD sum rules, which also support assigning the $Z_c(3900)$ to be the $J^{PC} = 1^{+-}$ diquark-antidiquark type tetraquark state. In Ref.[21], we take the diquark and antidiquark operators as the basic constituents to construct the scalar, axialvector and tensor currents to study the mass spectrum of the ground state hidden-charm tetraquark states with the QCD sum rules in a comprehensive way, and revisit the assignments of the $X(3860)$, $X(3872)$, $X(3915)$, $X(3940)$, $X(4160)$, $Z_c(3900)$, $Z_c(4020)$, $Z_c(4050)$, $Z_c(4055)$, $Z_c(4100)$, $Z_c(4200)$, $Z_c(4250)$, $Z_c(4430)$, $Z_c(4600)$, etc.

¹E-mail: zgwang@aliyun.com.

In those studies [7, 8, 19, 20, 21], the axialvector current,

$$J_\mu(x) = \frac{\varepsilon^{ijk}\varepsilon^{imn}}{\sqrt{2}} \left\{ u_j^T(x) C \gamma_5 c_k(x) \bar{d}_m(x) \gamma_\mu C \bar{c}_n^T(x) - u_j^T(x) C \gamma_\mu c_k(x) \bar{d}_m(x) \gamma_5 C \bar{c}_n^T(x) \right\}, \quad (1)$$

is chosen to interpolate the $Z_c(3900)$, where the i, j, k, m, n are color indices. The current $J_\mu(x)$ has the quantum numbers $J^{PC} = 1^{+-}$, the quantum field theory does not forbid the couplings to the two-particle scattering states $J/\psi\pi^+, \eta_c\rho^+, (D^*\bar{D}^*)^+, \dots$ with the $J^{PC} = 1^{+-}$. Up to now, the contributions of the two-particle scattering states in the QCD sum rules for the hidden-charm tetraquark states have not been studied quantitatively. On the other hand, there maybe exist a barrier or spatial separation between the diquark and antidiquark constituents [22, 23, 24, 25], the nonlocal effects have not been taken into account in the QCD sum rules for the tetraquark states yet. In this article, we study the $Z_c(3900)$ with the QCD sum rules in details by including the contributions of the two-particle scattering states and nonlocal effects between the diquark and antidiquark constituents, the conclusion is expected to survive for other diquark-antidiquark type tetraquark states.

The article is arranged as follows: in Sect.2, we derive the QCD sum rules by including the contributions of the two-particle scattering states and nonlocal effects between the diquark and antidiquark constituents; in Sect.3, we present the numerical results and discussions; and Sect.4 is reserved for our conclusion.

2 Two-particle contributions and nonlocal effects in the QCD sum rules

Firstly, we write down the two-point correlation function $\Pi_{\mu\nu}(p)$,

$$\Pi_{\mu\nu}(p) = i \int d^4x e^{ip \cdot x} \langle 0 | T \{ J_\mu(x, \epsilon) J_\nu^\dagger(0, \epsilon) \} | 0 \rangle, \quad (2)$$

where

$$J_\mu(x, \epsilon) = \frac{\varepsilon^{ijk}\varepsilon^{imn}}{\sqrt{2}} \left\{ \bar{d}_m(x + \epsilon) \gamma_\mu C \bar{c}_n^T(x + \epsilon) [x + \epsilon, x]^2 u_j^T(x) C \gamma_5 c_k(x) - \bar{d}_m(x + \epsilon) \gamma_5 C \bar{c}_n^T(x + \epsilon) [x + \epsilon, x]^2 u_j^T(x) C \gamma_\mu c_k(x) \right\}, \quad (3)$$

the i, j, k, m, n are color indices. The non-local current $J_\mu(x, \epsilon)$ is gauge-invariant due to the path-ordered gauge factor,

$$[x + \epsilon, x] = \text{P exp} \left[ig_s \int_x^{x+\epsilon} dy^\alpha G_\alpha(y) \right]. \quad (4)$$

We choose the current $J_\mu(x, \epsilon)$ to interpolate the $Z_c(3900)$, and take into account the nonlocal effects between the diquark and antidiquark constituents in the current $J_\mu(x, \epsilon)$ by adding a finite four vector ϵ . The diquark-antidiquark type tetraquark state can be plausibly described by two diquarks in a double well potential separated by a barrier [22, 23]. At long distances, the diquark and antidiquark serve as two point color charges, and attract each other strongly. At shorter distances, those effects beyond the naive one-gluon exchange force increase at decreasing distances and produce a repulsion between diquark and antidiquark constituents thus form a barrier to avoid destroying the diquark and antidiquark, if large enough [23]. The diquark-antidiquark type tetraquark states emerge as QCD molecular objects made of spatially separated colored two-quark lumps in the Born-Oppenheimer approximation [24]. In the dynamical picture of the tetraquark

states, the large spatial separation between the diquark and antidiquark leads to small wave-function overlap between the quark and antiquark constituents [25], which suppresses the Fierz rearrangements.

If we perform Fierz rearrangement both in the color and Dirac-spinor spaces, we can arrange the diquark-antidiquark type current $J_\mu(x, \epsilon)$ into a special superposition of the color-singlet-color-singlet type or meson-meson type currents [26, 27],

$$\begin{aligned} J_\mu &= \frac{1}{2\sqrt{2}} \left\{ i\bar{c}i\gamma_5 c \bar{d}\gamma_\mu u - i\bar{c}\gamma_\mu c \bar{d}i\gamma_5 u + \bar{c}u \bar{d}\gamma_\mu \gamma_5 c - \bar{c}\gamma_\mu \gamma_5 u \bar{d}c \right. \\ &\quad \left. - i\bar{c}\gamma^\nu \gamma_5 c \bar{d}\sigma_{\mu\nu} u + i\bar{c}\sigma_{\mu\nu} c \bar{d}\gamma^\nu \gamma_5 u - i\bar{c}\sigma_{\mu\nu} \gamma_5 u \bar{d}\gamma^\nu c + i\bar{c}\gamma^\nu u \bar{d}\sigma_{\mu\nu} \gamma_5 c \right\}, \\ &= \frac{1}{2\sqrt{2}} \left\{ iJ_\mu^1 - iJ_\mu^2 - iJ_\mu^3 + iJ_\mu^4 + J_\mu^5 - J_\mu^6 - iJ_\mu^7 + iJ_\mu^8 \right\}, \end{aligned} \quad (5)$$

where

$$\begin{aligned} J_\mu^1(x, \epsilon) &= \bar{c}(x+\epsilon)i\gamma_5 [x+\epsilon, x] c(x) \bar{d}(x+\epsilon)\gamma_\mu [x+\epsilon, x] u(x), \\ J_\mu^2(x, \epsilon) &= \bar{c}(x+\epsilon)\gamma_\mu [x+\epsilon, x] c(x) \bar{d}(x+\epsilon)i\gamma_5 [x+\epsilon, x] u(x), \\ J_\mu^3(x, \epsilon) &= \bar{c}(x+\epsilon)\gamma^\alpha \gamma_5 [x+\epsilon, x] c(x) \bar{d}(x+\epsilon)\sigma_{\mu\alpha} [x+\epsilon, x] u(x), \\ J_\mu^4(x, \epsilon) &= \bar{c}(x+\epsilon)\sigma_{\mu\alpha} [x+\epsilon, x] c(x) \bar{d}(x+\epsilon)\gamma^\alpha \gamma_5 [x+\epsilon, x] u(x), \\ J_\mu^5(x, \epsilon) &= \bar{c}(x+\epsilon) [x+\epsilon, x] u(x) \bar{d}(x+\epsilon)\gamma_\mu \gamma_5 [x+\epsilon, x] c(x), \\ J_\mu^6(x, \epsilon) &= \bar{c}(x+\epsilon)\gamma_\mu \gamma_5 [x+\epsilon, x] u(x) \bar{d}(x+\epsilon) [x+\epsilon, x] c(x), \\ J_\mu^7(x, \epsilon) &= \bar{c}(x+\epsilon)\sigma_{\mu\alpha} \gamma_5 [x+\epsilon, x] u(x) \bar{d}(x+\epsilon)\gamma^\alpha [x+\epsilon, x] c(x), \\ J_\mu^8(x, \epsilon) &= \bar{c}(x+\epsilon)\gamma^\alpha [x+\epsilon, x] u(x) \bar{d}(x+\epsilon)\sigma_{\mu\alpha} \gamma_5 [x+\epsilon, x] c(x). \end{aligned} \quad (6)$$

The currents $J_\mu^n(x, \epsilon)$ with $n = 1, 2, \dots, 8$ are gauge-invariant due to the path-ordered gauge factor $[x+\epsilon, x]$. In the following, we drop the gauge factors by taking the Fock-Schwinger gauge $y_\alpha G^\alpha(y) = 0$ in Eq.(4). In fact, the barrier or spatial separation between the diquark and antidiquark pair frustrates the Fierz rearrangements [22, 23, 24, 25].

We expand the currents $J_\mu(x, \epsilon)$ and $J_\mu^n(x, \epsilon)$ with $n = 1, 2, \dots, 8$ in terms of Taylor series of ϵ ,

$$\begin{aligned} J_\mu(x, \epsilon) &= J_\mu(x, 0) + \frac{\partial J_\mu(x, \epsilon)}{\partial \epsilon^\alpha} \Big|_{\epsilon=0} \epsilon^\alpha + \frac{1}{2} \frac{\partial^2 J_\mu(x, \epsilon)}{\partial \epsilon^\alpha \partial \epsilon^\beta} \Big|_{\epsilon=0} \epsilon^\alpha \epsilon^\beta + \dots, \\ J_\mu^n(x, \epsilon) &= J_\mu^n(x, 0) + \frac{\partial J_\mu^n(x, \epsilon)}{\partial \epsilon^\alpha} \Big|_{\epsilon=0} \epsilon^\alpha + \frac{1}{2} \frac{\partial^2 J_\mu^n(x, \epsilon)}{\partial \epsilon^\alpha \partial \epsilon^\beta} \Big|_{\epsilon=0} \epsilon^\alpha \epsilon^\beta + \dots, \end{aligned} \quad (7)$$

then expand the correlation function $\Pi_{\mu\nu}(p)$ also in terms of Taylor series of ϵ ,

$$\Pi_{\mu\nu}(p) = \Pi_{\mu\nu}(\mathcal{O}(\epsilon^0)) + \Pi_{\mu\nu}(\mathcal{O}(\epsilon^1)) + \Pi_{\mu\nu}(\mathcal{O}(\epsilon^2)) + \dots, \quad (8)$$

where the components $\Pi_{\mu\nu}(\mathcal{O}(\epsilon^i))$ with $i = 0, 1, 2, \dots$ represent the contributions of the order $\mathcal{O}(\epsilon^i)$. We write the contributions in the leading order explicitly,

$$\Pi_{\mu\nu}(\mathcal{O}(\epsilon^0)) = \Pi(p^2) \left(-g_{\mu\nu} + \frac{p_\mu p_\nu}{p^2} \right) + \Pi_0(p^2) \frac{p_\mu p_\nu}{p^2}, \quad (9)$$

according to Lorentz covariance, where the $\Pi(p^2)$ and $\Pi_0(p^2)$ denote the spin 1 and 0 components respectively. In this article, we study the component $\Pi(p^2)$.

In Ref.[7], we observe that the axialvector tetraquark current $J_\mu(x, 0)$ couples potentially to the $Z_c(3900)$,

$$\langle 0 | J_\mu(0, 0) | Z_c(p) \rangle = \lambda_Z \epsilon_\mu, \quad (10)$$

where the λ_Z is the current-hadron coupling constant or pole residue, the ε_μ is the polarization vector.

The color-singlet-color-singlet type currents couple potentially to the meson-meson pairs or molecular states. In the following, we write down the couplings to the meson-meson pairs explicitly,

$$\begin{aligned}
\langle 0|J_\mu^1(0,0)|\eta_c(q)\rho(p-q)\rangle &= \frac{f_{\eta_c}m_{\eta_c}^2}{2m_c}f_\rho m_\rho \varepsilon_\mu^\rho, \\
\langle 0|J_\mu^2(0,0)|\pi(q)J/\psi(p-q)\rangle &= \frac{f_\pi m_\pi^2}{m_u+m_d}f_{J/\psi}m_{J/\psi}\varepsilon_\mu^{J/\psi}, \\
\langle 0|J_\mu^2(0,0)|\pi(q)\psi'(p-q)\rangle &= \frac{f_\pi m_\pi^2}{m_u+m_d}f_{\psi'}m_{\psi'}\varepsilon_\mu^{\psi'}, \tag{11}
\end{aligned}$$

$$\begin{aligned}
\langle 0|J_\mu^3(0,0)|\eta_c(q)\rho(p-q)\rangle &= -if_{\eta_c}q^\alpha if_\rho^T [\varepsilon_\mu^\rho(p-q)_\alpha - \varepsilon_\alpha^\rho(p-q)_\mu], \\
\langle 0|J_\mu^3(0,0)|\eta_c(q)b_1(p-q)\rangle &= -if_{\eta_c}q^\alpha if_{b_1}\varepsilon_{\mu\alpha\sigma\tau}\varepsilon_{h_1}^\sigma(p-q)^\tau, \\
\langle 0|J_\mu^3(0,0)|\chi_{c1}(q)\rho(p-q)\rangle &= f_{\chi_{c1}}m_{\chi_{c1}}\varepsilon_{\chi_{c1}}^\alpha if_\rho^T [\varepsilon_\mu^\rho(p-q)_\alpha - \varepsilon_\alpha^\rho(p-q)_\mu], \tag{12}
\end{aligned}$$

$$\begin{aligned}
\langle 0|J_\mu^4(0,0)|\pi(q)J/\psi(p-q)\rangle &= -if_\pi q^\alpha if_{J/\psi}^T [\varepsilon_\mu^{J/\psi}(p-q)_\alpha - \varepsilon_\alpha^{J/\psi}(p-q)_\mu], \\
\langle 0|J_\mu^4(0,0)|\pi(q)\psi'(p-q)\rangle &= -if_\pi q^\alpha if_{\psi'}^T [\varepsilon_\mu^{\psi'}(p-q)_\alpha - \varepsilon_\alpha^{\psi'}(p-q)_\mu], \\
\langle 0|J_\mu^4(0,0)|\pi(q)h_c(p-q)\rangle &= -if_\pi q^\alpha if_{h_c}\varepsilon_{\mu\alpha\sigma\tau}\varepsilon_{h_c}^\sigma(p-q)^\tau, \\
\langle 0|J_\mu^4(0,0)|\pi(q)h'_c(p-q)\rangle &= -if_\pi q^\alpha if_{h'_c}\varepsilon_{\mu\alpha\sigma\tau}\varepsilon_{h'_c}^\sigma(p-q)^\tau, \\
\langle 0|J_\mu^4(0,0)|a_1(q)J/\psi(p-q)\rangle &= f_{a_1}m_{a_1}\varepsilon_{a_1}^\alpha if_{J/\psi}^T [\varepsilon_\mu^{J/\psi}(p-q)_\alpha - \varepsilon_\alpha^{J/\psi}(p-q)_\mu], \tag{13}
\end{aligned}$$

$$\begin{aligned}
\langle 0|J_\mu^{5/6}(0,0)|\bar{D}_0(q)D(p-q)\rangle &= -if_{D_0}m_{D_0}f_D(p-q)_\mu, \\
\langle 0|J_\mu^{7/8}(0,0)|\bar{D}^*(q)D^*(p-q)\rangle &= f_{D^*}m_{D^*}\varepsilon_{D^*}^\alpha if_{D^*}^T \varepsilon_{\mu\alpha\sigma\tau}\varepsilon_{D^*}^\sigma(p-q)^\tau, \\
\langle 0|J_\mu^{7/8}(0,0)|\bar{D}_0(q)D^*(p-q)\rangle &= f_{D_0}q^\alpha if_{D^*}^T \varepsilon_{\mu\alpha\sigma\tau}\varepsilon_{D^*}^\sigma(p-q)^\tau, \tag{14}
\end{aligned}$$

the ε_μ are the polarization vectors of the vector and axialvector mesons, the f_{η_c} , f_ρ , f_ρ^T , f_π , $f_{J/\psi}$, $f_{\psi'}$, $f_{J/\psi}^T$, $f_{\psi'}^T$, f_{h_c} , $f_{h'_c}$, f_{b_1} , $f_{\chi_{c1}}$, f_{a_1} , f_{D_0} , f_D , f_{D^*} and $f_{D^*}^T$ are the decay constants.

At the hadron side, we take into account the contributions of the tetraquark candidate $Z_c(3900)$ and the two-particle scattering state contributions from the $\pi J/\psi$, πh_c , $\eta_c \rho$, $D^* D^*$, $D_0 D$, $\eta_c b_1$, $\chi_{c1} \rho$, $a_1 J/\psi$, $D_0 D^*$, $\pi \psi'$, $\pi h'_c$, $\pi \psi''$ below the threshold of the $Z_c(4430)$, which can be assigned to the first radial excitation of the $Z_c(3900)$ [15, 16, 17],

$$\begin{aligned}
\Pi(p^2) &= \frac{\lambda_Z^2}{M_Z^2 - p^2} \\
&+ \lambda_{\eta_c \rho; 11}^2 \int_{m_{\eta_c \rho}^2}^{s_0} ds \frac{1}{s - p^2} \frac{\sqrt{\lambda(s, m_{\eta_c}^2, m_\rho^2)}}{s} \left[1 + \frac{\lambda(s, m_{\eta_c}^2, m_\rho^2)}{12sm_\rho^2} \right] \\
&+ \lambda_{\pi J/\psi; 22}^2 \int_{m_{\pi J/\psi}^2}^{s_0} ds \frac{1}{s - p^2} \frac{\sqrt{\lambda(s, m_\pi^2, m_{J/\psi}^2)}}{s} \left[1 + \frac{\lambda(s, m_\pi^2, m_{J/\psi}^2)}{12sm_{J/\psi}^2} \right] \\
&+ \frac{\lambda_{\eta_c \rho; 33}^2}{4} \int_{m_{\eta_c \rho}^2}^{s_0} ds \frac{1}{s - p^2} \frac{\sqrt{\lambda(s, m_{\eta_c}^2, m_\rho^2)}}{s} \left[(s - m_{\eta_c}^2 - m_\rho^2)^2 - \frac{\lambda(s, m_{\eta_c}^2, m_\rho^2)(s - m_\rho^2)}{3s} \right]
\end{aligned}$$

$$\begin{aligned}
& + \frac{\lambda_{\pi J/\psi;44}^2}{4} \int_{m_{\pi J/\psi}^2}^{s_0} ds \frac{1}{s-p^2} \frac{\sqrt{\lambda(s, m_\pi^2, m_{J/\psi}^2)}}{s} \left[(s - m_\pi^2 - m_{J/\psi}^2)^2 - \frac{\lambda(s, m_\pi^2, m_{J/\psi}^2)(s - m_{J/\psi}^2)}{3s} \right] \\
& + \lambda_{\eta_c \rho;13}^2 \int_{m_{\eta_c \rho}^2}^{s_0} ds \frac{1}{s-p^2} \frac{\sqrt{\lambda(s, m_{\eta_c}^2, m_\rho^2)}}{s} \left[\frac{\lambda(s, m_{\eta_c}^2, m_\rho^2)}{6} - (s - m_{\eta_c}^2 - m_\rho^2) \right] \\
& + \lambda_{\pi J/\psi;24}^2 \int_{m_{\pi J/\psi}^2}^{s_0} ds \frac{1}{s-p^2} \frac{\sqrt{\lambda(s, m_\pi^2, m_{J/\psi}^2)}}{s} \left[\frac{\lambda(s, m_\pi^2, m_{J/\psi}^2)}{6} - (s - m_\pi^2 - m_{J/\psi}^2) \right] \\
& + \lambda_{\eta_c b_1;33}^2 \int_{m_{\eta_c b_1}^2}^{s_0} ds \frac{1}{s-p^2} \frac{\sqrt{\lambda(s, m_{\eta_c}^2, m_{b_1}^2)}}{s} \frac{\lambda(s, m_{\eta_c}^2, m_{b_1}^2)}{6} \\
& + \lambda_{\chi_{c1} \rho;33}^2 \int_{m_{\chi_{c1} \rho}^2}^{s_0} ds \frac{1}{s-p^2} \frac{\sqrt{\lambda(s, m_{\chi_{c1}}^2, m_\rho^2)}}{s} \frac{\lambda(s, m_{\chi_{c1}}^2, m_\rho^2)(2s + m_\rho^2 + 2m_{\chi_{c1}}^2)}{12sm_{\chi_{c1}}^2} \\
& + \lambda_{\pi h_c;44}^2 \int_{m_{\pi h_c}^2}^{s_0} ds \frac{1}{s-p^2} \frac{\sqrt{\lambda(s, m_\pi^2, m_{h_c}^2)}}{s} \frac{\lambda(s, m_\pi^2, m_{h_c}^2)}{6} \\
& + \lambda_{a_1 J/\psi;44}^2 \int_{m_{a_1 J/\psi}^2}^{s_0} ds \frac{1}{s-p^2} \frac{\sqrt{\lambda(s, m_{a_1}^2, m_{J/\psi}^2)}}{s} \frac{\lambda(s, m_{a_1}^2, m_{J/\psi}^2)(2s + m_{J/\psi}^2 + 2m_{a_1}^2)}{12sm_{a_1}^2} \\
& + \lambda_{D_0 D;55/66}^2 \int_{m_{D_0 D}^2}^{s_0} ds \frac{1}{s-p^2} \frac{\sqrt{\lambda(s, m_{D_0}^2, m_D^2)}}{s} \frac{\lambda(s, m_{D_0}^2, m_D^2)}{12s} \\
& + \lambda_{D^* D^*;77/88}^2 \int_{m_{D^* D^*}^2}^{s_0} ds \frac{1}{s-p^2} \frac{\sqrt{\lambda(s, m_{D^*}^2, m_{D^*}^2)}}{s} \left[2m_{D^*}^2 + \frac{\lambda(s, m_{D^*}^2, m_{D^*}^2)(s + m_{D^*}^2)}{6sm_{D^*}^2} \right] \\
& + \lambda_{D_0 D^*;77/88}^2 \int_{m_{D_0 D^*}^2}^{s_0} ds \frac{1}{s-p^2} \frac{\sqrt{\lambda(s, m_{D_0}^2, m_{D^*}^2)}}{s} \frac{\lambda(s, m_{D_0}^2, m_{D^*}^2)}{6} \\
& + \lambda_{\pi \psi';22}^2 \int_{m_{\pi \psi'}^2}^{s_0} ds \frac{1}{s-p^2} \frac{\sqrt{\lambda(s, m_\pi^2, m_{\psi'}^2)}}{s} \left[1 + \frac{\lambda(s, m_\pi^2, m_{\psi'}^2)}{12sm_{\psi'}^2} \right] \\
& + \frac{\lambda_{\pi \psi';44}^2}{4} \int_{m_{\pi \psi'}^2}^{s_0} ds \frac{1}{s-p^2} \frac{\sqrt{\lambda(s, m_\pi^2, m_{\psi'}^2)}}{s} \left[(s - m_\pi^2 - m_{\psi'}^2)^2 - \frac{\lambda(s, m_\pi^2, m_{\psi'}^2)(s - m_{\psi'}^2)}{3s} \right] \\
& + \lambda_{\pi \psi';24}^2 \int_{m_{\pi \psi'}^2}^{s_0} ds \frac{1}{s-p^2} \frac{\sqrt{\lambda(s, m_\pi^2, m_{\psi'}^2)}}{s} \left[\frac{\lambda(s, m_\pi^2, m_{\psi'}^2)}{6} - (s - m_\pi^2 - m_{\psi'}^2) \right] \\
& + \lambda_{\pi h_c';44}^2 \int_{m_{\pi h_c'}^2}^{s_0} ds \frac{1}{s-p^2} \frac{\sqrt{\lambda(s, m_\pi^2, m_{h_c'}^2)}}{s} \frac{\lambda(s, m_\pi^2, m_{h_c'}^2)}{6} \\
& + (\pi \psi' \rightarrow \pi \psi'') + \dots,
\end{aligned} \tag{15}$$

where

$$\begin{aligned}\lambda_{\eta_c \rho; 11}^2 &= \frac{1}{128\pi^2} \frac{f_{\eta_c}^2 m_{\eta_c}^4 f_{\rho}^2 m_{\rho}^2}{4m_c^2}, \\ \lambda_{\pi J/\psi; 22}^2 &= \frac{1}{128\pi^2} \frac{f_{\pi}^2 m_{\pi}^4 f_{J/\psi}^2 m_{J/\psi}^2}{(m_u + m_d)^2},\end{aligned}\tag{16}$$

$$\begin{aligned}\lambda_{\eta_c \rho; 33}^2 &= \frac{1}{128\pi^2} f_{\eta_c}^2 f_{\rho}^{T2}, \\ \lambda_{\eta_c b_1; 33}^2 &= \frac{1}{128\pi^2} f_{\eta_c}^2 f_{b_1}^2, \\ \lambda_{\chi_{c1} \rho; 33}^2 &= \frac{1}{128\pi^2} f_{\chi_{c1}}^2 m_{\chi_{c1}}^2 f_{\rho}^{T2},\end{aligned}\tag{17}$$

$$\begin{aligned}\lambda_{\pi J/\psi; 44}^2 &= \frac{1}{128\pi^2} f_{\pi}^2 f_{J/\psi}^{T2}, \\ \lambda_{\pi h_c; 44}^2 &= \frac{1}{128\pi^2} f_{\pi}^2 f_{h_c}^2, \\ \lambda_{a_1 J/\psi; 44}^2 &= \frac{1}{128\pi^2} f_{a_1}^2 m_{a_1}^2 f_{J/\psi}^{T2},\end{aligned}\tag{18}$$

$$\begin{aligned}\lambda_{\eta_c \rho; 13}^2 &= \frac{1}{128\pi^2} \frac{f_{\eta_c}^2 m_{\eta_c}^2 f_{\rho} m_{\rho} f_{\rho}^T}{2m_c}, \\ \lambda_{\pi J/\psi; 24}^2 &= \frac{1}{128\pi^2} \frac{f_{\pi}^2 m_{\pi}^2 f_{J/\psi} m_{J/\psi} f_{J/\psi}^T}{m_u + m_d},\end{aligned}\tag{19}$$

$$\begin{aligned}\lambda_{D_0 D; 55/66}^2 &= \frac{1}{128\pi^2} f_{D_0}^2 m_{D_0}^2 f_D^2, \\ \lambda_{D^* D^*; 77/88}^2 &= \frac{1}{128\pi^2} f_{D^*}^2 m_{D^*}^2 f_{D^*}^{T2}, \\ \lambda_{D_0 D^*; 77/88}^2 &= \frac{1}{128\pi^2} f_{D_0}^2 f_{D^*}^{T2},\end{aligned}\tag{20}$$

$$\begin{aligned}\lambda_{\psi'; 22}^2 &= \frac{1}{128\pi^2} \frac{f_{\pi}^2 m_{\pi}^4 f_{\psi'}^2 m_{\psi'}^2}{(m_u + m_d)^2}, \\ \lambda_{\pi \psi'; 44}^2 &= \frac{1}{128\pi^2} f_{\pi}^2 f_{\psi'}^{T2}, \\ \lambda_{\pi \psi'; 24}^2 &= \frac{1}{128\pi^2} \frac{f_{\pi}^2 m_{\pi}^2 f_{\psi'} m_{\psi'} f_{\psi'}^T}{m_u + m_d}, \\ \lambda_{\pi h'_c; 44}^2 &= \frac{1}{128\pi^2} f_{\pi}^2 f_{h'_c}^2,\end{aligned}\tag{21}$$

$\lambda(a, b, c) = a^2 + b^2 + c^2 - 2ab - 2ac - 2bc$, $m_{\eta_c \rho}^2 = (m_{\eta_c} + m_{\rho})^2$, $m_{\pi J/\psi}^2 = (m_{\pi} + m_{J/\psi})^2$, $m_{\eta_c b_1}^2 = (m_{\eta_c} + m_{b_1})^2$, $m_{\pi h_c}^2 = (m_{\pi} + m_{h_c})^2$, $m_{\chi_{c1} \rho}^2 = (m_{\chi_{c1}} + m_{\rho})^2$, $m_{a_1 J/\psi}^2 = (m_{a_1} + m_{J/\psi})^2$, $m_{D_0 D}^2 = (m_{D_0} + m_D)^2$, $m_{D^* D^*}^2 = (m_{D^*} + m_{D^*})^2$, $m_{D_0 D^*}^2 = (m_{D_0} + m_{D^*})^2$, $m_{\pi \psi'}^2 = (m_{\pi} + m_{\psi'})^2$, $m_{\pi h'_c}^2 = (m_{\pi} + m_{h'_c})^2$, the continuum threshold parameter $\sqrt{s_0} \leq M_{Z_c(4430)}$. In Table 1, we present the thresholds for the relevant meson-meson pairs from the Particle Data Group [4].

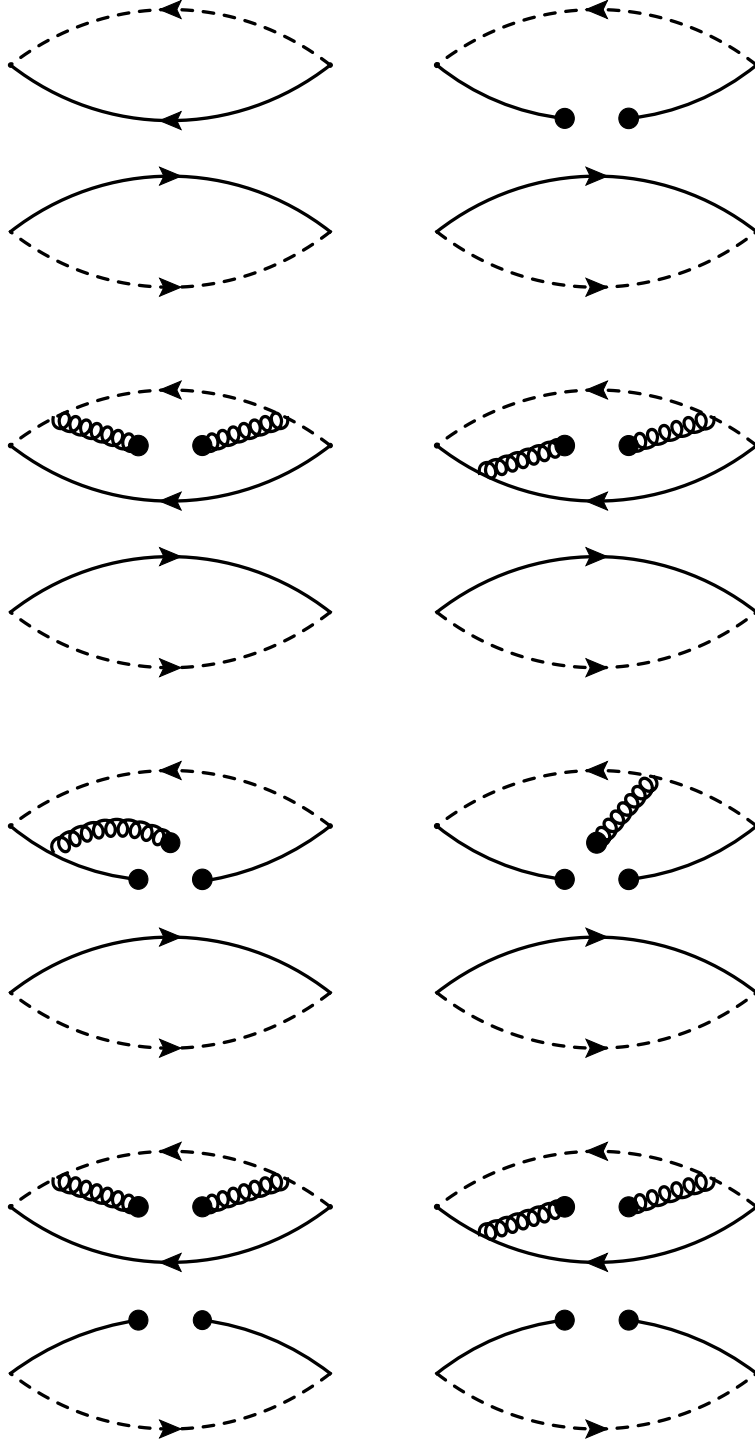


Figure 1: The factorizable Feynman diagrams contribute to the perturbative term, $\langle \bar{q}q \rangle$, $\langle \frac{\alpha_s GG}{\pi} \rangle$, $\langle \bar{q}g_s \sigma G q \rangle$ and $\langle \bar{q}q \rangle \langle \frac{\alpha_s GG}{\pi} \rangle$, where the solid lines and dashed lines denote the light quarks and heavy quarks, respectively. Other diagrams obtained by interchanging of the light quark lines and heavy quark lines are implied.

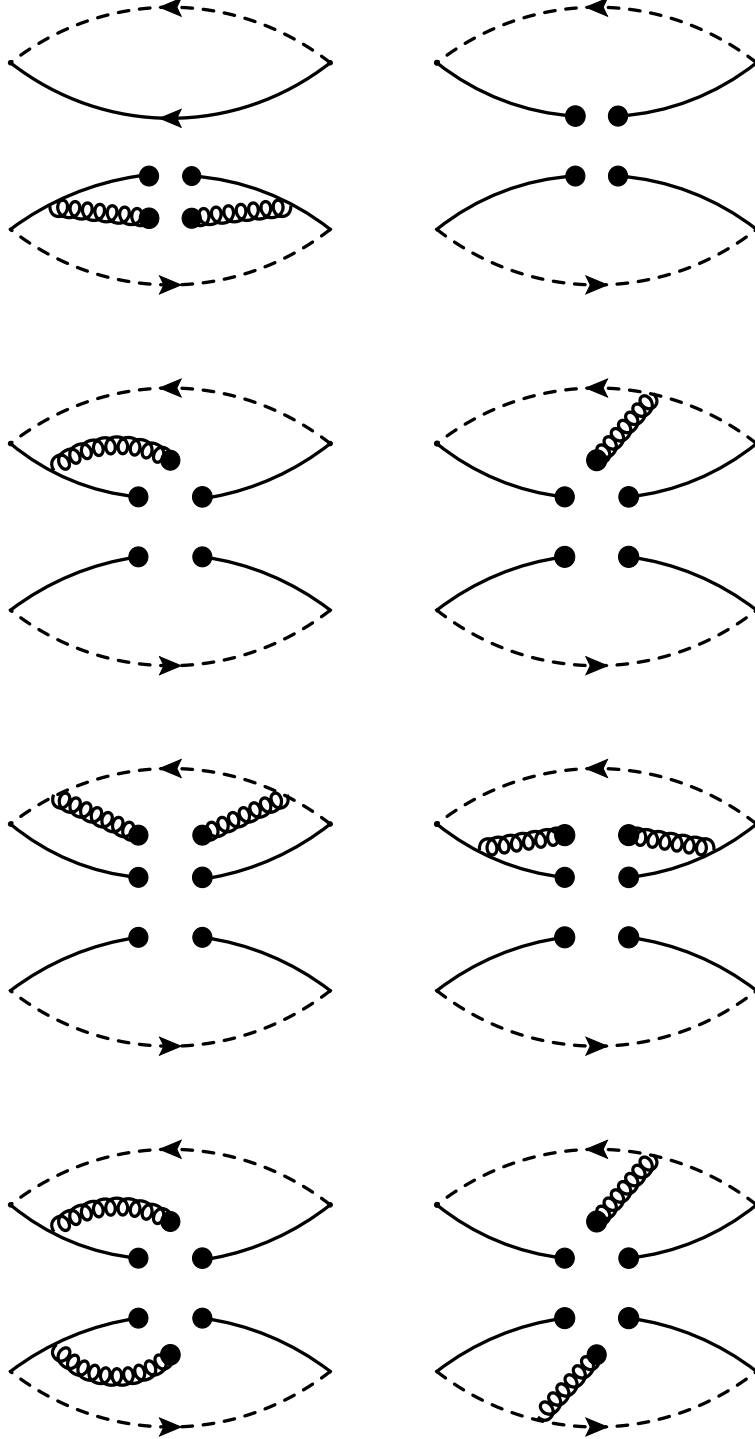


Figure 2: The factorizable Feynman diagrams contribute to the $\langle \bar{q}q \rangle \langle \frac{\alpha_s GG}{\pi} \rangle$, $\langle \bar{q}q \rangle^2$, $\langle \bar{q}q \rangle \langle \bar{q}g_s \sigma Gq \rangle$, $\langle \bar{q}q \rangle^2 \langle \frac{\alpha_s GG}{\pi} \rangle$ and $\langle \bar{q}g_s \sigma Gq \rangle^2$. Other diagrams obtained by interchanging of the light quark lines and heavy quark lines are implied.

	$\pi J/\psi$	πh_c	$\eta_c \rho$	$D^* D^*$	$D_0 D$	$\eta_c b_1$	$\chi_{c1} \rho$	$a_1 J/\psi$	$D_0 D^*$
Thresholds (GeV)	3.24	3.67	3.76	4.02	4.19	4.21	4.29	4.33	4.33
	$\pi \psi'$	$\pi \psi''$	$\pi h'_c$						
Thresholds (GeV)	3.83	4.12	4.10						

Table 1: The thresholds for the relevant meson-meson pairs from the Particle Data Group.

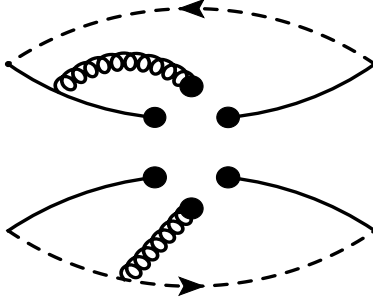


Figure 3: The factorizable Feynman diagrams contribute to the $\langle \bar{q} g_s \sigma G q \rangle^2$. Other diagrams obtained by interchanging of the light quark lines and heavy quark lines are implied.

At the QCD side, the correlation function $\Pi_{\mu\nu}(p)$ of the order $\mathcal{O}(\epsilon^0)$ can be written as

$$\begin{aligned}
\Pi_{\mu\nu}(p) = & -\frac{i\epsilon^{ijk}\epsilon^{lmn}\epsilon^{i'j'k'}\epsilon^{i'm'n'}}{2} \int d^4x e^{ip \cdot x} \\
& \left\{ \text{Tr} \left[\gamma_5 C^{kk'}(x) \gamma_5 C U^{jj'T}(x) C \right] \text{Tr} \left[\gamma_\nu C^{m'n}(-x) \gamma_\mu C D^{m'mT}(-x) C \right] \right. \\
& + \text{Tr} \left[\gamma_\mu C^{kk'}(x) \gamma_\nu C U^{jj'T}(x) C \right] \text{Tr} \left[\gamma_5 C^{m'n}(-x) \gamma_5 C D^{m'mT}(-x) C \right] \\
& + \text{Tr} \left[\gamma_\mu C^{kk'}(x) \gamma_5 C U^{jj'T}(x) C \right] \text{Tr} \left[\gamma_\nu C^{m'n}(-x) \gamma_5 C D^{m'mT}(-x) C \right] \\
& \left. + \text{Tr} \left[\gamma_5 C^{kk'}(x) \gamma_\nu C U^{jj'T}(x) C \right] \text{Tr} \left[\gamma_5 C^{m'n}(-x) \gamma_\mu C D^{m'mT}(-x) C \right] \right\}, \quad (22)
\end{aligned}$$

where the $U_{ij}(x)$, $D_{ij}(x)$ and $C_{ij}(x)$ are the full u , d and c quark propagators respectively ($S_{ij}(x) = U_{ij}(x)$, $D_{ij}(x)$),

$$\begin{aligned}
S_{ij}(x) = & \frac{i\delta_{ij}\not{x}}{2\pi^2 x^4} - \frac{\delta_{ij}\langle \bar{q}q \rangle}{12} - \frac{\delta_{ij}x^2\langle \bar{q}g_s\sigma Gq \rangle}{192} - \frac{ig_s G_{\alpha\beta}^a t_{ij}^a (\not{x}\sigma^{\alpha\beta} + \sigma^{\alpha\beta}\not{x})}{32\pi^2 x^2} \\
& - \frac{\delta_{ij}x^4\langle \bar{q}q \rangle\langle g_s^2 GG \rangle}{27648} - \frac{1}{8}\langle \bar{q}_j\sigma^{\mu\nu}q_i \rangle\sigma_{\mu\nu} + \dots, \quad (23)
\end{aligned}$$

$$\begin{aligned}
C_{ij}(x) = & \frac{i}{(2\pi)^4} \int d^4k e^{-ik \cdot x} \left\{ \frac{\delta_{ij}}{k - m_c} - \frac{g_s G_{\alpha\beta}^n t_{ij}^n}{4} \frac{\sigma^{\alpha\beta}(k + m_c) + (k + m_c)\sigma^{\alpha\beta}}{(k^2 - m_c^2)^2} \right. \\
& \left. - \frac{g_s^2(t^a t^b)_{ij} G_{\alpha\beta}^a G_{\mu\nu}^b (f^{\alpha\beta\mu\nu} + f^{\alpha\mu\beta\nu} + f^{\alpha\mu\nu\beta})}{4(k^2 - m_c^2)^5} + \dots \right\}, \\
f^{\alpha\beta\mu\nu} = & (k + m_c)\gamma^\alpha(k + m_c)\gamma^\beta(k + m_c)\gamma^\mu(k + m_c)\gamma^\nu(k + m_c), \quad (24)
\end{aligned}$$

and $t^n = \frac{\lambda^n}{2}$, the λ^n is the Gell-Mann matrix [7, 28, 29].

As there exists a spatial separation ϵ between the diquark and antiquark constituents, we

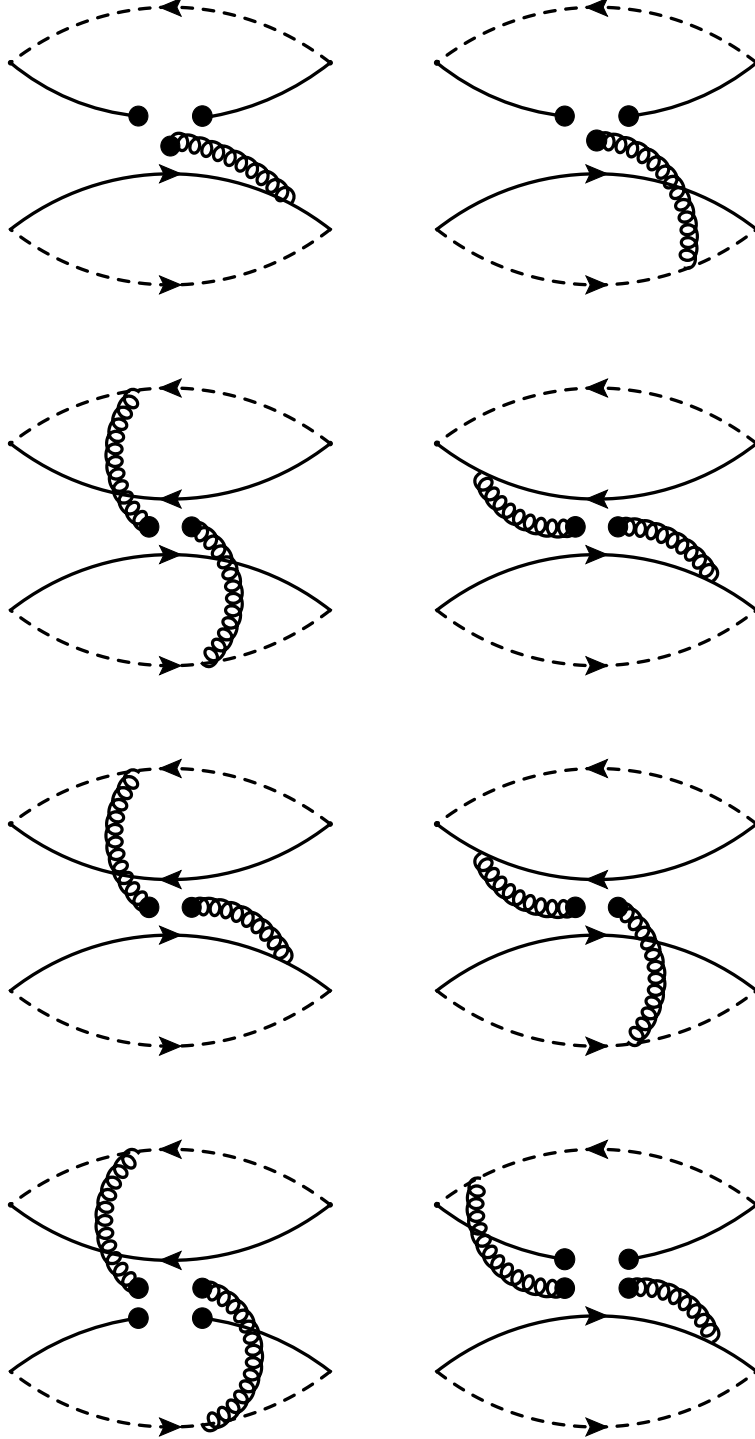


Figure 4: The nonfactorizable Feynman diagrams contribute to the $\langle \bar{q}g_s\sigma Gq \rangle$, $\langle \frac{\alpha_s GG}{\pi} \rangle$ and $\langle \bar{q}q \rangle \langle \frac{\alpha_s GG}{\pi} \rangle$. Other diagrams obtained by interchanging of the light quark lines and heavy quark lines are implied.

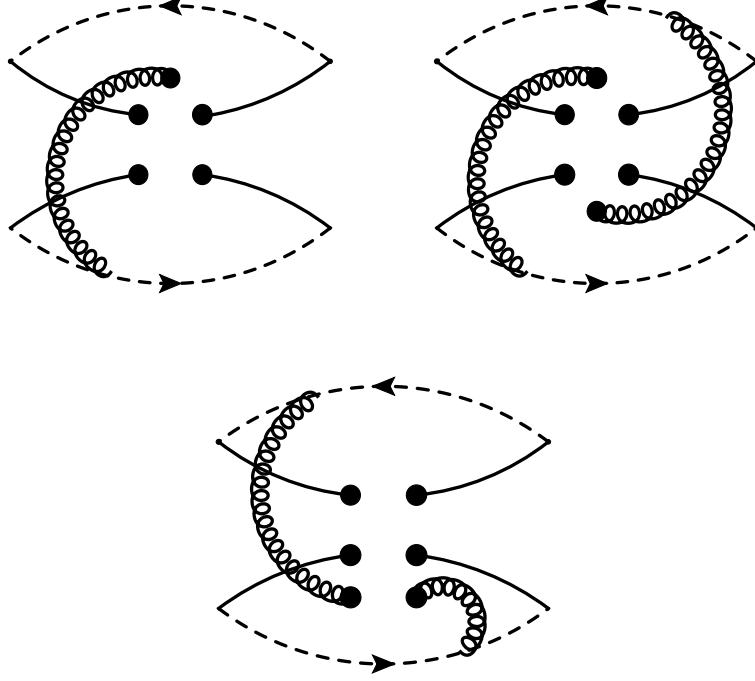


Figure 5: The nonfactorizable Feynman diagrams contribute to the $\langle \bar{q}q \rangle \langle \bar{q}g_s \sigma Gq \rangle$, $\langle \bar{q}g_s \sigma Gq \rangle^2$ and $\langle \bar{q}q \rangle^2 \langle \frac{\alpha_s GG}{\pi} \rangle$. Other diagrams obtained by interchanging of the light quark lines and heavy quark lines are implied.

split the point 0 (and x) into two points,

$$\begin{aligned} 0 &\rightarrow 0, 0 + \epsilon, \\ x &\rightarrow x, x + \epsilon, \end{aligned} \quad (25)$$

to distinguish the diquark and antidiquark contributions in drawing the Feynman diagrams according to Eq.(22). We classify the Feynman diagrams as factorizable diagrams and nonfactorizable diagrams respectively. In Figs.1-3, we draw the factorizable Feynman diagrams, in which the contributions come from the diquark loops and antidiquark loops are factorizable due to the nonzero spatial separation ϵ . They contribute to the perturbative terms, $\langle \bar{q}q \rangle$, $\langle \bar{q}g_s \sigma Gq \rangle$, $\langle \frac{\alpha_s GG}{\pi} \rangle$, $\langle \bar{q}q \rangle^2$, $\langle \bar{q}q \rangle \langle \frac{\alpha_s GG}{\pi} \rangle$, $\langle \bar{q}q \rangle \langle \bar{q}g_s \sigma Gq \rangle$, $\langle \bar{q}q \rangle^2 \langle \frac{\alpha_s GG}{\pi} \rangle$ and $\langle \bar{q}g_s \sigma Gq \rangle^2$. In Figs.4-5, we draw the nonfactorizable Feynman diagrams, in which the contributions come from the diquark loops and antidiquark loops are nonfactorizable even if we take into account the nonzero spatial separation ϵ . They contribute to the $\langle \bar{q}g_s \sigma Gq \rangle$, $\langle \frac{\alpha_s GG}{\pi} \rangle$, $\langle \bar{q}q \rangle \langle \frac{\alpha_s GG}{\pi} \rangle$, $\langle \bar{q}q \rangle \langle \bar{q}g_s \sigma Gq \rangle$, $\langle \bar{q}q \rangle^2 \langle \frac{\alpha_s GG}{\pi} \rangle$ and $\langle \bar{q}g_s \sigma Gq \rangle^2$.

We compute both the factorizable and nonfactorizable Feynman diagrams, and obtain the correlation function $\Pi(p^2)$ at the quark level, then obtain the QCD spectral density through dispersion relation. We match the hadron side with the QCD side of the correlation function $\Pi(p^2)$ below the continuum threshold parameter s_0 , then perform the Borel transformation with respect to the variable $P^2 = -p^2$ to obtain the QCD sum rules,

$$\lambda_Z^2 \exp\left(-\frac{M_Z^2}{T^2}\right) + \Pi_{\text{RC}}(T^2) = \int_{4m_c^2}^{s_0} ds \left[\rho_f(s) + \rho_{nf}(s) \right] \exp\left(-\frac{s}{T^2}\right), \quad (26)$$

where the two particle scattering state contributions (RC),

$$\begin{aligned}
\Pi_{\text{RC}}(T^2) = & \lambda_{\eta_c \rho; 11}^2 \int_{m_{\eta_c \rho}^2}^{s_0} ds \frac{\sqrt{\lambda(s, m_{\eta_c}^2, m_{\rho}^2)}}{s} \left[1 + \frac{\lambda(s, m_{\eta_c}^2, m_{\rho}^2)}{12sm_{\rho}^2} \right] \exp\left(-\frac{s}{T^2}\right) \\
& + \lambda_{\pi J/\psi; 22}^2 \int_{m_{\pi J/\psi}^2}^{s_0} ds \frac{\sqrt{\lambda(s, m_{\pi}^2, m_{J/\psi}^2)}}{s} \left[1 + \frac{\lambda(s, m_{\pi}^2, m_{J/\psi}^2)}{12sm_{J/\psi}^2} \right] \exp\left(-\frac{s}{T^2}\right) \\
& + \frac{\lambda_{\eta_c \rho; 33}^2}{4} \int_{m_{\eta_c \rho}^2}^{s_0} ds \frac{\sqrt{\lambda(s, m_{\eta_c}^2, m_{\rho}^2)}}{s} \left[(s - m_{\eta_c}^2 - m_{\rho}^2)^2 - \frac{\lambda(s, m_{\eta_c}^2, m_{\rho}^2)(s - m_{\rho}^2)}{3s} \right] \exp\left(-\frac{s}{T^2}\right) \\
& + \frac{\lambda_{\pi J/\psi; 44}^2}{4} \int_{m_{\pi J/\psi}^2}^{s_0} ds \frac{\sqrt{\lambda(s, m_{\pi}^2, m_{J/\psi}^2)}}{s} \left[(s - m_{\pi}^2 - m_{J/\psi}^2)^2 - \frac{\lambda(s, m_{\pi}^2, m_{J/\psi}^2)(s - m_{J/\psi}^2)}{3s} \right] \exp\left(-\frac{s}{T^2}\right) \\
& + \lambda_{\eta_c \rho; 13}^2 \int_{m_{\eta_c \rho}^2}^{s_0} ds \frac{\sqrt{\lambda(s, m_{\eta_c}^2, m_{\rho}^2)}}{s} \left[\frac{\lambda(s, m_{\eta_c}^2, m_{\rho}^2)}{6} - (s - m_{\eta_c}^2 - m_{\rho}^2) \right] \exp\left(-\frac{s}{T^2}\right) \\
& + \lambda_{\pi J/\psi; 24}^2 \int_{m_{\pi J/\psi}^2}^{s_0} ds \frac{\sqrt{\lambda(s, m_{\pi}^2, m_{J/\psi}^2)}}{s} \left[\frac{\lambda(s, m_{\pi}^2, m_{J/\psi}^2)}{6} - (s - m_{\pi}^2 - m_{J/\psi}^2) \right] \exp\left(-\frac{s}{T^2}\right) \\
& + \lambda_{\eta_c b_1; 33}^2 \int_{m_{\eta_c b_1}^2}^{s_0} ds \frac{\sqrt{\lambda(s, m_{\eta_c}^2, m_{b_1}^2)}}{s} \frac{\lambda(s, m_{\eta_c}^2, m_{b_1}^2)}{6} \exp\left(-\frac{s}{T^2}\right) \\
& + \lambda_{\chi_{c1} \rho; 33}^2 \int_{m_{\chi_{c1} \rho}^2}^{s_0} ds \frac{\sqrt{\lambda(s, m_{\chi_{c1}}^2, m_{\rho}^2)}}{s} \frac{\lambda(s, m_{\chi_{c1}}^2, m_{\rho}^2)(2s + m_{\rho}^2 + 2m_{\chi_{c1}}^2)}{12sm_{\chi_{c1}}^2} \exp\left(-\frac{s}{T^2}\right) \\
& + \lambda_{\pi h_c; 44}^2 \int_{m_{\pi h_c}^2}^{s_0} ds \frac{\sqrt{\lambda(s, m_{\pi}^2, m_{h_c}^2)}}{s} \frac{\lambda(s, m_{\pi}^2, m_{h_c}^2)}{6} \exp\left(-\frac{s}{T^2}\right) \\
& + \lambda_{a_1 J/\psi; 44}^2 \int_{m_{a_1 J/\psi}^2}^{s_0} ds \frac{\sqrt{\lambda(s, m_{a_1}^2, m_{J/\psi}^2)}}{s} \frac{\lambda(s, m_{a_1}^2, m_{J/\psi}^2)(2s + m_{J/\psi}^2 + 2m_{a_1}^2)}{12sm_{a_1}^2} \exp\left(-\frac{s}{T^2}\right) \\
& + \lambda_{D_0 D; 55/66}^2 \int_{m_{D_0 D}^2}^{s_0} ds \frac{\sqrt{\lambda(s, m_{D_0}^2, m_D^2)}}{s} \frac{\lambda(s, m_{D_0}^2, m_D^2)}{12s} \exp\left(-\frac{s}{T^2}\right) \\
& + \lambda_{D^* D^*; 77/88}^2 \int_{m_{D^* D^*}^2}^{s_0} ds \frac{\sqrt{\lambda(s, m_{D^*}^2, m_{D^*}^2)}}{s} \left[2m_{D^*}^2 + \frac{\lambda(s, m_{D^*}^2, m_{D^*}^2)(s + m_{D^*}^2)}{6sm_{D^*}^2} \right] \exp\left(-\frac{s}{T^2}\right) \\
& + \lambda_{D_0 D^*; 77/88}^2 \int_{m_{D_0 D^*}^2}^{s_0} ds \frac{\sqrt{\lambda(s, m_{D_0}^2, m_{D^*}^2)}}{s} \frac{\lambda(s, m_{D_0}^2, m_{D^*}^2)}{6} \exp\left(-\frac{s}{T^2}\right) \\
& + \lambda_{\pi \psi'; 22}^2 \int_{m_{\pi \psi'}^2}^{s_0} ds \frac{\sqrt{\lambda(s, m_{\pi}^2, m_{\psi'}^2)}}{s} \left[1 + \frac{\lambda(s, m_{\pi}^2, m_{\psi'}^2)}{12sm_{\psi'}^2} \right] \exp\left(-\frac{s}{T^2}\right) \\
& + \frac{\lambda_{\pi \psi'; 44}^2}{4} \int_{m_{\pi \psi'}^2}^{s_0} ds \frac{\sqrt{\lambda(s, m_{\pi}^2, m_{\psi'}^2)}}{s} \left[(s - m_{\pi}^2 - m_{\psi'}^2)^2 - \frac{\lambda(s, m_{\pi}^2, m_{\psi'}^2)(s - m_{\psi'}^2)}{3s} \right] \exp\left(-\frac{s}{T^2}\right)
\end{aligned}$$

$$\begin{aligned}
& + \lambda_{\pi\psi';24}^2 \int_{m_{\pi\psi'}^2}^{s_0} ds \frac{\sqrt{\lambda(s, m_\pi^2, m_{\psi'}^2)}}{s} \left[\frac{\lambda(s, m_\pi^2, m_{\psi'}^2)}{6} - (s - m_\pi^2 - m_{\psi'}^2) \right] \exp\left(-\frac{s}{T^2}\right) \\
& + \lambda_{\pi h_c;44}^2 \int_{m_{\pi h_c'}^2}^{s_0} ds \frac{\sqrt{\lambda(s, m_\pi^2, m_{h_c'}^2)}}{s} \frac{\lambda(s, m_\pi^2, m_{h_c'}^2)}{6} \exp\left(-\frac{s}{T^2}\right) + (\pi\psi' \rightarrow \pi\psi'') , \quad (27)
\end{aligned}$$

the QCD spectral densities $\rho_f(s)$ and $\rho_{nf}(s)$ receive contributions from the factorizable and nonfactorizable Feynman diagrams, respectively. The explicit expressions of the QCD spectral densities $\rho_f(s)$ and $\rho_{nf}(s)$ are available upon request by contacting me via E-mail.

If there exists a barrier or spatial separation between the diquark and antidiquark constituents, the Feynman diagrams can be divided into factorizable and nonfactorizable diagrams. The factorizable Feynman diagrams correspond to the stable diquark-antidiquark type contributions. The barrier or spatial separation frustrates dissociation of the diquark and antidiquark states to form the color singlet quark-antiquark pairs $q\bar{q}$, $Q\bar{Q}$ or $Q\bar{q}$, $q\bar{Q}$, the colored diquark and antidiquark constituents are confined objects, which lead to a stable tetraquark state. The nonfactorizable Feynman diagrams correspond to the tunnelling effects between diquark and antidiquark constituents, and facilitate dissociation of the diquark and antidiquark states to form the color singlet quark-antiquark pairs $q\bar{q}$, $Q\bar{Q}$ or $Q\bar{q}$, $q\bar{Q}$. In this case, the QCD sum rules in Eq.(26) can be replaced with two QCD sum rules,

$$\lambda_Z^2 \exp\left(-\frac{M_Z^2}{T^2}\right) = \int_{4m_c^2}^{s_0} ds \rho_f(s) \exp\left(-\frac{s}{T^2}\right), \quad (28)$$

$$\Pi_{\text{RC}}(T^2) = \int_{4m_c^2}^{s_0} ds \rho_{nf}(s) \exp\left(-\frac{s}{T^2}\right). \quad (29)$$

On the other hand, if the effects of the barrier or spatial separation between the diquark and antidiquark constituents are neglectful, we can perform Fierz rearrangement for the diquark-antidiquark type current in the color and Dirac-spinor spaces freely to obtain a special superposition of the color-singlet-color-singlet type or meson-meson type currents, which couple potentially to the meson-meson pairs, it is not necessary to take into account the pole term of the $Z_c(3900)$, in other words, the axialvector tetraquark state does not exist as a real resonance, it is a virtual state and embodies the net effects. And it is not necessary to divide the Feynman diagrams into factorizable and nonfactorizable parts. We saturate the hadron side of the QCD sum rules with the two-particle scattering state contributions,

$$\Pi_{\text{RC}}(T^2) = \kappa \int_{4m_c^2}^{s_0} ds \left[\rho_f(s) + \rho_{nf}(s) \right] \exp\left(-\frac{s}{T^2}\right), \quad (30)$$

where we introduce a parameter κ to measure the deviation from the ideal value 1.

We derive Eq.(26), Eq.(28) and Eq.(30) with respect to $\tau = \frac{1}{T^2}$, and obtain the QCD sum rules for the tetraquark mass and other QCD sum rules,

$$M_Z^2 = \frac{-\frac{d}{d\tau} \left\{ \int_{4m_c^2}^{s_0} ds \left[\rho_f(s) + \rho_{nf}(s) \right] \exp\left(-\frac{s}{T^2}\right) - \Pi_{\text{RC}}(T^2) \right\}}{\int_{4m_c^2}^{s_0} ds \left[\rho_f(s) + \rho_{nf}(s) \right] \exp\left(-\frac{s}{T^2}\right) - \Pi_{\text{RC}}(T^2)} \Big|_{\tau=\frac{1}{T^2}}, \quad (31)$$

$$M_Z^2 = \frac{-\frac{d}{d\tau} \int_{4m_c^2}^{s_0} ds \rho_f(s) \exp\left(-\frac{s}{T^2}\right)}{\int_{4m_c^2}^{s_0} ds \rho_f(s) \exp\left(-\frac{s}{T^2}\right)} \Big|_{\tau=\frac{1}{T^2}}, \quad (32)$$

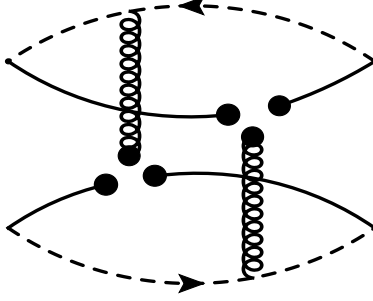


Figure 6: The connected Feynman diagrams contribute to the vacuum condensates $\langle \bar{q}g_s\sigma Gq \rangle^2$ for the meson-meson type currents.

$$\frac{d}{d\tau}\Pi_{\text{RC}}(T^2) = \kappa \frac{d}{d\tau} \int_{4m_c^2}^{s_0} ds \left[\rho_f(s) + \rho_{nf}(s) \right] \exp\left(-\frac{s}{T^2}\right) \Big|_{\tau=\frac{1}{T^2}}. \quad (33)$$

For the meson-meson type currents, Lucha, Melikhov and Sazdjian argue that the connected Feynman diagrams appear at the order $\mathcal{O}(\alpha_s^2)$, and contribute to a Landau pole or a branch cut to approve the existence of the tetraquark (molecular) state or an adequate QCD sum rule, the disconnected Feynman diagrams at the order $\mathcal{O}(\alpha_s^k)$ with $k \leq 1$ correspond to the meson-meson-like contributions [30, 31]. If the arguments of Lucha, Melikhov and Sazdjian are right, only the two QCD sum rules shown in Eq.(30) and Eq.(33) survive in the present case.

The vacuum condensates serve as a landmark for the nonperturbative nature of the QCD sum rules, the connected contributions in the case of meson-meson type currents appear at the order $\mathcal{O}(\alpha_s)$ due to the operators $\bar{q}g_sGq\bar{q}g_sGq$, which come from the Feynman diagrams shown in Fig.6 and lead to the vacuum condensate $\langle \bar{q}g_s\sigma Gq \rangle^2$, those contributions are of the order $\mathcal{O}(\alpha_s^0)$ as a matter of fact. The tetraquark molecular states begin to receive connected contributions at the order $\mathcal{O}(\alpha_s^0)$, not at the order $\mathcal{O}(\alpha_s^2)$ asserted in Refs.[30, 31].

The quarks and gluons are confined objects, they cannot be put on the mass-shell, it is questionable to assert that the Landau equation is applicable in the nonperturbative calculations exploring the four-quark bound states [32]. The Landau pole does not mean that there exists a tetraquark (molecular) state, because the Landau pole is merely a kinematical singularity, not a dynamical singularity [33].

We should bear in mind that the Landau equation requires pole masses rather than \overline{MS} masses to ensure that there exist mass poles or mass-shells in pure perturbative calculations. For the heavy quarks, the pole masses are $\hat{m}_c = 1.67 \pm 0.07$ GeV and $\hat{m}_b = 4.78 \pm 0.06$ GeV from the Particle Data Group [4], the thresholds $2\hat{m}_c = 3.34 \pm 0.14$ GeV $> m_{\eta_c}, m_{J/\psi}$, and $2\hat{m}_b = 9.56 \pm 0.12$ GeV $> m_{\eta_b}, m_{\Upsilon}$. It is unreliable that the masses of the ground state charmonium (bottomonium) states lie below the threshold $2\hat{m}_c$ ($2\hat{m}_b$) in the QCD sum rules for the η_c and J/ψ (η_b and Υ).

In Refs.[30, 31], Lucha, Melikhov and Sazdjian only obtain formal QCD sum rules for the tetraquark (molecular) states, not obtain feasible QCD sum rules with predictions can be confronted to the experimental data. For the meson-meson type currents, it is reasonable to take the viewpoint that the disconnected Feynman diagrams give masses to the meson-meson pair, while the connected Feynman diagrams contribute weak attractive interactions to bind the massive meson-meson pair to form loosely molecular states.

3 Numerical results and discussions

At the QCD side, we take the standard values of the vacuum condensates $\langle \bar{q}q \rangle = -(0.24 \pm 0.01 \text{ GeV})^3$, $\langle \bar{q}g_s\sigma Gq \rangle = m_0^2 \langle \bar{q}q \rangle$, $m_0^2 = (0.8 \pm 0.1) \text{ GeV}^2$, $\langle \frac{\alpha_s GG}{\pi} \rangle = (0.33 \text{ GeV})^4$ at the energy

scale $\mu = 1 \text{ GeV}$ [28, 34, 35], and choose the \overline{MS} mass $m_c(m_c) = (1.275 \pm 0.025) \text{ GeV}$ from the Particle Data Group [4]. Moreover, we take into account the energy-scale dependence of the parameters,

$$\begin{aligned}
\langle \bar{q}q \rangle(\mu) &= \langle \bar{q}q \rangle(1 \text{ GeV}) \left[\frac{\alpha_s(1 \text{ GeV})}{\alpha_s(\mu)} \right]^{\frac{12}{25}}, \\
\langle \bar{q}g_s \sigma G q \rangle(\mu) &= \langle \bar{q}g_s \sigma G q \rangle(1 \text{ GeV}) \left[\frac{\alpha_s(1 \text{ GeV})}{\alpha_s(\mu)} \right]^{\frac{2}{25}}, \\
m_c(\mu) &= m_c(m_c) \left[\frac{\alpha_s(\mu)}{\alpha_s(m_c)} \right]^{\frac{12}{25}}, \\
\alpha_s(\mu) &= \frac{1}{b_0 t} \left[1 - \frac{b_1}{b_0^2} \frac{\log t}{t} + \frac{b_1^2 (\log^2 t - \log t - 1) + b_0 b_2}{b_0^4 t^2} \right], \tag{34}
\end{aligned}$$

where $t = \log \frac{\mu^2}{\Lambda^2}$, $b_0 = \frac{33-2n_f}{12\pi}$, $b_1 = \frac{153-19n_f}{24\pi^2}$, $b_2 = \frac{2857 - \frac{5033}{9}n_f + \frac{325}{27}n_f^2}{128\pi^3}$, $\Lambda = 210 \text{ MeV}$, 292 MeV and 332 MeV for the flavors $n_f = 5, 4$ and 3 , respectively [4, 36], and evolve all the parameters to the ideal energy scale μ with $n_f = 4$ to extract the axialvector tetraquark mass as the c -quark is concerned.

At the hadron side, we take the hadronic parameters as $m_{\eta_c} = 2.9839 \text{ GeV}$, $m_{J/\psi} = 3.0969 \text{ GeV}$, $m_{h_c} = 3.5254 \text{ GeV}$, $m_{\chi_{c1}} = 3.5107 \text{ GeV}$, $m_\rho = 0.7753 \text{ GeV}$, $m_{a_1} = 1.2300 \text{ GeV}$, $m_{b_1} = 1.2295 \text{ GeV}$, $m_\pi = 0.1396 \text{ GeV}$, $m_D = 1.8672 \text{ GeV}$, $m_{D^*} = 2.0086 \text{ GeV}$, $m_{D_0} = 2.3245 \text{ GeV}$, $m_{\psi'} = 3.6861 \text{ GeV}$, $m_{\psi''} = 4.0396 \text{ GeV}$ from the Particle Data Group [4]; $m_{h'_c} = 3.9560 \text{ GeV}$ for the Godfrey-Isgur model [37], $f_{J/\psi} = 0.418 \text{ GeV}$, $f_{\eta_c} = 0.387 \text{ GeV}$, $f_{J/\psi}^T = 0.410 \text{ GeV}$, $f_{h_c} = 0.235 \text{ GeV}$ from Lattice QCD [38]; $f_{\chi_{c1}} = 0.338 \text{ GeV}$ [39], $f_\rho = 0.205 \text{ GeV}$, $f_\rho^T = 0.160 \text{ GeV}$ [40], $f_{b_1} = 0.180 \text{ GeV}$ [41], $f_{a_1} = 0.238 \text{ GeV}$ [42], $f_D = 0.208 \text{ GeV}$, $f_{D^*} = 0.263 \text{ GeV}$, $f_{D_0} = 0.373 \text{ GeV}$ [43] from the QCD sum rules; $f_\pi = 0.130 \text{ GeV}$, $f_{\psi'} = 0.295 \text{ GeV}$, $f_{\psi''} = 0.187 \text{ GeV}$ extracted from the experimental data [4]; $f_{D^*}^T = f_{D^*}$, $f_{\psi'}^T = f_{\psi'}$, $f_{\psi''}^T = f_{\psi''}$, $f_{h'_c} = f_{h_c} \frac{f_{\psi'}}{f_{J/\psi}} = 0.166 \text{ GeV}$ estimated in the present work; $f_\pi m_\pi^2 / (m_u + m_d) = -2\langle \bar{q}q \rangle / f_\pi$ from the Gell-Mann-Oakes-Renner relation. In the present work, we take the average values of the charged and neutral D mesons.

We choose the values of the decay constants from the lattice QCD, the QCD sum rules or extracted from the experimental data, where the perturbative corrections have been taken into account. In the present work, we obtain the expressions of the QCD spectral densities $\rho_f(s)$ and $\rho_{nf}(s)$ at the leading order, the value of the $\Pi_{\text{RC}}(T^2)$ at the hadron side is overestimated. At the leading order, $\bar{f}_D = 0.170 \text{ GeV}$, $\bar{f}_{D^*} = 0.240 \text{ GeV}$ [44]. The $\Pi_{\text{RC}}(T^2) \propto f_M^4$, where the M denotes the mesons. At the leading order, we can take the replacement $\Pi_{\text{RC}}(T^2) \rightarrow \bar{\Pi}_{\text{RC}}(T^2) = \Pi_{\text{RC}}(T^2) \frac{\bar{f}_M^4}{f_M^4}$. Considering the ratios $\frac{\bar{f}_D^4}{f_D^4} = 0.45$ and $\frac{\bar{f}_{D^*}^4}{f_{D^*}^4} = 0.69$, we multiply the $\Pi_{\text{RC}}(T^2)$ by a factor 0.7 to subtract the perturbative corrections mildly, $\bar{\Pi}_{\text{RC}}(T^2) = 0.7 \Pi_{\text{RC}}(T^2)$.

3.1 $Z_c(3900)$ plus two-particle scattering states

From Table 1, we can see that the largest thresholds are $m_{a_1 J/\psi}$ and $m_{D_0 D^*}$. We take into account the large widths of the scalar D mesons, $\Gamma_{D_0^0} = 274 \pm 40 \text{ MeV}$ and $\Gamma_{D_0^\pm} = 221 \pm 18 \text{ MeV}$ [4], and choose the continuum threshold parameter as $\sqrt{s_0} = M_{Z_c} + 0.55 \text{ GeV} = 4.45 \text{ GeV}$ according to mass gaps $M_{Z_c(4430)} - M_{Z_c(3900)} = m_{\psi'} - m_{J/\psi} = 589 \text{ MeV}$ [4]. Furthermore, we add a uncertainty 0.1 GeV . If only the $Z_c(3900)$ is retained, we can choose a slightly smaller continuum threshold parameter $\sqrt{s_0} = M_{Z_c} + 0.50 \pm 0.1 \text{ GeV} = 4.40 \text{ GeV}$. At the optimal energy scale $\mu = 1.4 \text{ GeV}$

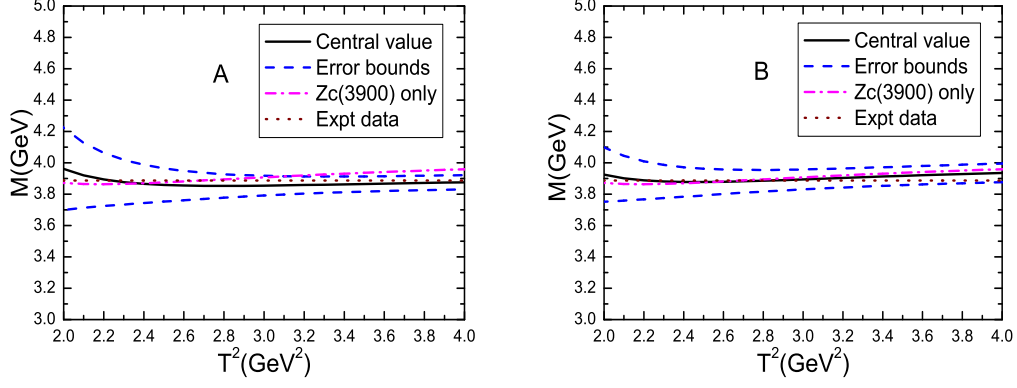


Figure 7: The mass of the $Z_c(3900)$ with variations of the Borel parameter T^2 , where the A and B correspond to the $\Pi_{RC}(T^2)$ and $\bar{\Pi}_{RC}(T^2)$, respectively.

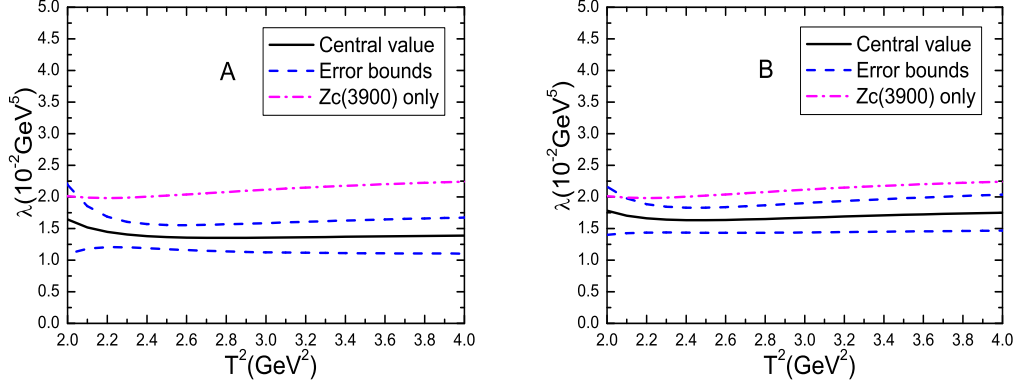


Figure 8: The pole residue of the $Z_c(3900)$ with variations of the Borel parameter T^2 , where the A and B correspond to the $\Pi_{RC}(T^2)$ and $\bar{\Pi}_{RC}(T^2)$, respectively.

[21], the pole contribution (PC) is,

$$\begin{aligned}
 \text{PC} &= \frac{\int_{4m_c^2}^{s_0} ds \left[\rho_f(s) + \rho_{nf}(s) \right] \exp\left(-\frac{s}{T^2}\right)}{\int_{4m_c^2}^{\infty} ds \left[\rho_f(s) + \rho_{nf}(s) \right] \exp\left(-\frac{s}{T^2}\right)} \\
 &= (43 - 66)\%,
 \end{aligned} \tag{35}$$

at the Borel window $T^2 = (2.7 - 3.1) \text{ GeV}$. The pole dominance criterion is well satisfied. On the other hand, the contributions of the vacuum condensates of dimension 10 are less than 1%, the operator product expansion is well convergent.

We take into account the uncertainties of the input parameters, and obtain the values of the

mass and pole residue, which are shown explicitly in Figs.7-8,

$$\begin{aligned} M_Z &= 3.85 \pm 0.09 \text{ GeV}, \\ \lambda_Z &= (1.35 \pm 0.24) \times 10^{-2} \text{ GeV}^5 \text{ with } \Pi_{\text{RC}}(T^2), \end{aligned} \quad (36)$$

$$\begin{aligned} M_Z &= 3.89 \pm 0.08 \text{ GeV}, \\ \lambda_Z &= (1.66 \pm 0.25) \times 10^{-2} \text{ GeV}^5 \text{ with } \bar{\Pi}_{\text{RC}}(T^2). \end{aligned} \quad (37)$$

Although the values of the mass are both in consistent with the experimental data $M_{Z_c(3900)} = (3887.2 \pm 2.3) \text{ MeV}$ from the Particle Data Group [4], the value $M_Z = 3.89 \pm 0.08 \text{ GeV}$ with the $\bar{\Pi}_{\text{RC}}(T^2)$ is better. In Figs.7-8, we plot the mass and pole residue with variations of the Borel parameter T^2 at much larger range than the Borel window.

If we switch off the two-particle scattering state contributions $\Pi_{\text{RC}}(T^2)$, we can obtain the values,

$$\begin{aligned} M_Z &= 3.90 \pm 0.08 \text{ GeV}, \\ \lambda_Z &= (2.09 \pm 0.33) \times 10^{-2} \text{ GeV}^5. \end{aligned} \quad (38)$$

Compared with the value $M_Z = 3.90 \pm 0.08 \text{ GeV}$ from the single-pole approximation [21], the values $M_Z = 3.85 \pm 0.09 \text{ GeV}$ and $3.89 \pm 0.08 \text{ GeV}$ from the QCD sum rules where the two-particle scattering state contributions included are slightly smaller, see Fig.7. While the values of the pole residue $\lambda_Z = (1.35 \pm 0.24) \times 10^{-2} \text{ GeV}^5$ and $(1.66 \pm 0.25) \times 10^{-2} \text{ GeV}^5$ are much smaller than the value $(2.09 \pm 0.33) \times 10^{-2} \text{ GeV}^5$ from the single-pole approximation, see Fig.8. In all the QCD sum rules, there appear Borel platforms in the Bore window $T^2 = (2.7 - 3.1) \text{ GeV}^2$. Moreover, the energy scale formula $\mu = \sqrt{M_{X/Y/Z}^2 - (2\mathbb{M}_c)^2}$ with the updated effective c -quark mass $\mathbb{M}_c = 1.82 \text{ GeV}$ [26, 45] is satisfied for the QCD sum rules with or without the two-particle scattering state contributions $\bar{\Pi}_{\text{RC}}(T^2)$, as the $\Pi_{\text{RC}}(T^2)$ overestimates the two-particle scattering state contributions. All in all, the pole contribution of the $Z_c(3900)$ is necessary, the current $J_\mu(x)$ couples potentially to the $Z_c(3900)$.

3.2 Two-particle contributions only

Again we choose the continuum threshold parameter $\sqrt{s_0} = 4.45 \pm 0.10 \text{ GeV}$ and the optimal energy scale $\mu = 1.4 \text{ GeV}$, the pole contribution is $\text{PC} = (43 - 66)\%$ at the Borel window $T^2 = (2.7 - 3.1) \text{ GeV}^2$. As there are only the two-particle scattering state contributions, the QCD sum rules are reduced to two independent QCD sum rules in Eq.(30) and Eq.(33).

We take into account the uncertainties of the input parameters, and obtain the values of the κ , which are shown explicitly in Fig.9,

$$\begin{aligned} \kappa &= 0.55 \pm 0.11 \text{ from Eq.(30)}, \\ &= 0.57 \pm 0.11 \text{ from Eq.(33)}, \end{aligned} \quad (39)$$

in the Borel window. If we take the replacement $\Pi_{\text{RC}}(T^2) \rightarrow \bar{\Pi}_{\text{RC}}(T^2)$ to subtract the perturbative corrections, we obtain the corresponding values $\bar{\kappa}$,

$$\begin{aligned} \bar{\kappa} &= 0.39 \pm 0.08 \text{ from Eq.(30)}, \\ &= 0.40 \pm 0.08 \text{ from Eq.(33)}. \end{aligned} \quad (40)$$

The values $\kappa, \bar{\kappa} \ll 1$, the two-particle scattering state contributions cannot saturate the QCD sum rules at the hadron side. If we insist on performing the Fierz rearrangement,

$$J_\mu = \frac{1}{2\sqrt{2}} \left\{ iJ_\mu^1 - iJ_\mu^2 - iJ_\mu^3 + iJ_\mu^4 + J_\mu^5 - J_\mu^6 - iJ_\mu^7 + iJ_\mu^8 \right\}, \quad (41)$$

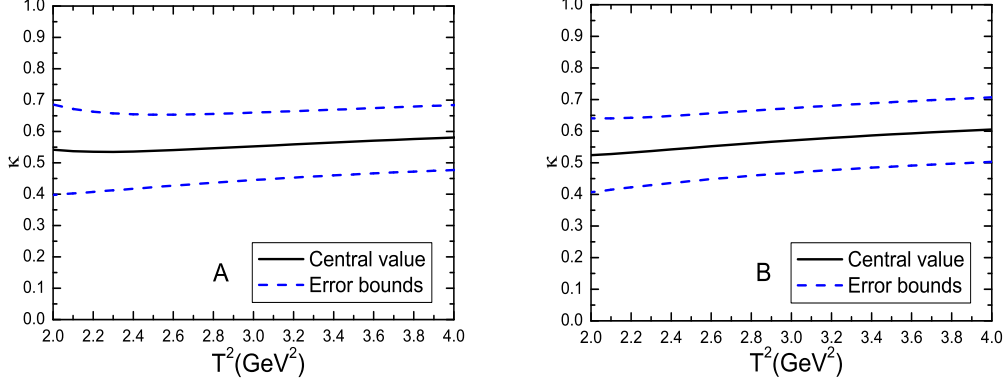


Figure 9: The κ with variations of the Borel parameter T^2 , where the A and B correspond to the QCD sum rules in Eq.(30) and Eq.(33), respectively.

we should take into account the possible molecular states, such as $\eta_c \rho$, $\pi J/\psi$, \dots ,

$$\begin{aligned} \langle 0 | J_\mu^1(0, 0) | \eta_c \rho(p) \rangle &= \lambda_{\eta_c \rho, M} \varepsilon_\mu, \\ \langle 0 | J_\mu^2(0, 0) | \pi J/\psi(p) \rangle &= \lambda_{\pi J/\psi, M} \varepsilon_\mu, \end{aligned} \quad (42)$$

\dots , where the $\lambda_{\eta_c \rho, M}$, $\lambda_{\pi J/\psi, M}$, \dots are the pole residues, the ε_μ are the polarization vectors. All in all, the two-particle scattering state contributions cannot saturate the QCD sum rules.

For the meson-meson type currents, Lucha, Melikhov and Sazdjian argue that the disconnected Feynman diagrams at the order $\mathcal{O}(\alpha_s^k)$ with $k \leq 1$ correspond to the meson-meson-like contributions [30, 31], which lead to the two QCD sum rules shown in Eq.(30) and Eq.(33) in the present case. However, the small values κ , $\bar{\kappa} \ll 1$ reject those arguments. The tetraquark (molecular) states have to be taken into account in the QCD sum rules, and they begin to receive contributions at the order $\mathcal{O}(\alpha_s^0)$.

3.3 $Z_c(3900)$ only with the factorizable Feynman diagrams

We choose the continuum threshold parameter $\sqrt{s_0} = 4.40 \pm 0.10$ GeV and the optimal energy scale $\mu = 1.4$ GeV, the pole contribution is $\text{PC} = (40 - 63)\%$ at the Borel window $T^2 = (2.7 - 3.1)$ GeV with both the factorizable and nonfactorizable Feynman diagrams.

In Fig.10, we plot the contribution from nonfactorizable Feynman diagrams with variations of the Borel parameter T^2 . From the figure, we can see that the nonfactorizable contribution is about 1% at the Borel window and play a minor important role in the QCD sum rules. No stable QCD sum rules can be obtained in Eq.(29). The dominance contributions come from the factorizable Feynman diagrams. The factorizable contributions consist of two colored clusters, a diquark cluster and an antidiquark cluster, the color confinement frustrates tunnelling effects and leads to stable tetraquark state, which is consistent with the small width of the $Z_c(3900)$.

From the QCD sum rules in Eq.(28) and Eq.(32), we can obtain the values of the mass and pole residue,

$$\begin{aligned} M_Z &= 3.90 \pm 0.08 \text{ GeV}, \\ \lambda_Z &= (2.09 \pm 0.33) \times 10^{-2} \text{ GeV}^5, \end{aligned} \quad (43)$$

the nonfactorizable contributions can be neglected safely in the Borel window.

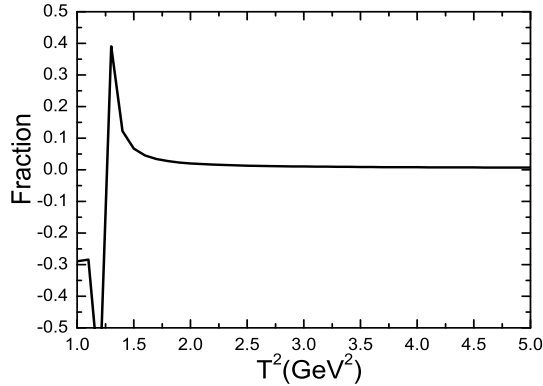


Figure 10: The contribution from nonfactorizable Feynman diagrams with variations of the Borel parameter T^2 .

4 Conclusion

In this article, we study the $Z_c(3900)$ with the QCD sum rules in details by including the contributions of the two-particle scattering states and nonlocal effects between the diquark and antiquark constituents. The two-particle scattering state contributions alone cannot saturate the QCD sum rules at the hadron side, we have to take into account the pole contribution of the $Z_c(3900)$. If we approximate the hadron side of the QCD sum rules with the $Z_c(3900)$ plus two-particle scattering state contributions, we can obtain a mass which is consistent with the experimental data. In fact, we can saturate the QCD sum rules with or without the two-particle scattering state contributions, although different pole residues are needed. If there exists a barrier or spatial separation between the diquark and antiquark constituents, the Feynman diagrams can be divided into the factorizable and nonfactorizable diagrams. The factorizable contributions consist of two colored clusters, a diquark cluster and an antiquark cluster, the color confinement frustrates tunnelling effects and leads to a stable tetraquark state, which is consistent with the small width of the $Z_c(3900)$. The nonfactorizable Feynman diagrams correspond to the tunnelling effects, which play a minor important role in the QCD sum rules. If we equal the nonfactorizable contributions to the two-particle scattering state contributions, no stable QCD sum rules can be obtained. The factorizable contributions dominate the QCD sum rules at the QCD side. The present conclusion is expected to survive in other QCD sum rules for the diquark-antiquark type tetraquark states. It is feasible to apply the QCD sum rules to study the tetraquark states, which begin to receive contributions at the order $\mathcal{O}(\alpha_s^0)$, not at the order $\mathcal{O}(\alpha_s^2)$.

Acknowledgements

This work is supported by National Natural Science Foundation, Grant Number 11775079.

References

- [1] M. Ablikim et al, Phys. Rev. Lett. **110** (2013) 252001.
- [2] Z. Q. Liu et al, Phys. Rev. Lett. **110** (2013) 252002.
- [3] T. Xiao, S. Dobbs, A. Tomaradze and K. K. Seth, Phys. Lett. **B727** (2013) 366.

- [4] M. Tanabashi et al, Phys. Rev. **D98** (2018) 030001.
- [5] R. Faccini, L. Maiani, F. Piccinini, A. Pilloni, A. D. Polosa and V. Riquer, Phys. Rev. **D87** (2013) 111102(R).
- [6] M. Karliner and S. Nussinov, JHEP **1307** (2013) 153; N. Mahajan, arXiv:1304.1301; E. Braaten, Phys. Rev. Lett. **111** (2013) 162003; C. F. Qiao and L. Tang, Eur. Phys. J. **C74** (2014) 3122.
- [7] Z. G. Wang and T. Huang, Phys. Rev. **D89** (2014) 054019.
- [8] J. M. Dias, F. S. Navarra, M. Nielsen and C. M. Zanetti, Phys. Rev. **D88** (2013) 016004.
- [9] F. K. Guo, C. Hidalgo-Duque, J. Nieves and M. P. Valderrama, Phys. Rev. **D88** (2013) 054007; J. R. Zhang, Phys. Rev. **D87** (2013) 116004; Y. Dong, A. Faessler, T. Gutsche and V. E. Lyubovitskij, Phys. Rev. **D88** (2013) 014030; H. W. Ke, Z. T. Wei and X. Q. Li, Eur. Phys. J. **C73** (2013) 2561; S. Prelovsek and L. Leskovec, Phys. Lett. **B727** (2013) 172; C. Y. Cui, Y. L. Liu, W. B. Chen and M. Q. Huang, J. Phys. **G41** (2014) 075003.
- [10] Z. G. Wang and T. Huang, Eur. Phys. J. **C74** (2014) 2891.
- [11] M. B. Voloshin, Phys. Rev. **D87** (2013) 091501.
- [12] D. Y. Chen, X. Liu and T. Matsuki, Phys. Rev. Lett. **110** (2013) 232001; Q. Wang, C. Hanhart and Q. Zhao, Phys. Rev. Lett. **111** (2013) 132003; X. H. Liu and G. Li, Phys. Rev. **D88** (2013) 014013.
- [13] R. Aaij et al, Phys. Rev. Lett. **112** (2014) 222002.
- [14] M. Ablikim et al, Phys. Rev. Lett. **119** (2017) 072001.
- [15] L. Maiani, F. Piccinini, A. D. Polosa and V. Riquer, Phys. Rev. **D89** (2014) 114010.
- [16] M. Nielsen and F. S. Navarra, Mod. Phys. Lett. **A29** (2014) 1430005.
- [17] Z. G. Wang, Commun. Theor. Phys. **63** (2015) 325.
- [18] S. S. Agaev, K. Azizi and H. Sundu, Phys. Rev. **D96** (2017) 034026.
- [19] S. S. Agaev, K. Azizi and H. Sundu, Phys. Rev. **D93** (2016) 074002.
- [20] Z. G. Wang and J. X. Zhang, Eur. Phys. J. **C78** (2018) 14.
- [21] Z. G. Wang, arXiv:1908.07914.
- [22] A. Selem and F. Wilczek, hep-ph/0602128.
- [23] L. Maiani, A. D. Polosa and V. Riquer, Phys. Lett. **B778** (2018) 247.
- [24] L. Maiani, A. D. Polosa and V. Riquer, Phys. Rev. **D100** (2019) 014002.
- [25] S. J. Brodsky, D. S. Hwang and R. F. Lebed, Phys. Rev. Lett. **113** (2014) 112001.
- [26] Z. G. Wang, Eur. Phys. J. **C74** (2014) 2874.
- [27] Z. G. Wang, Commun. Theor. Phys. **63** (2015) 466.
- [28] L. J. Reinders, H. Rubinstein and S. Yazaki, Phys. Rept. **127** (1985) 1.
- [29] P. Pascual and R. Tarrach, “QCD: Renormalization for the practitioner”, Springer Berlin Heidelberg (1984).

- [30] W. Lucha, D. Melikhov and H. Sazdjian, Phys. Rev. **D100** (2019) 014010; W. Lucha, D. Melikhov and H. Sazdjian, Phys. Rev. **D100** (2019) 074029.
- [31] W. Lucha, D. Melikhov and H. Sazdjian, Eur. Phys. J. **C77** (2017) 866.
- [32] L. D. Landau, Nucl. Phys. **13** (1959) 181.
- [33] F. K. Guo, X. H. Liu and S. Sakai, arXiv:1912.07030.
- [34] M. A. Shifman, A. I. Vainshtein and V. I. Zakharov, Nucl. Phys. **B147** (1979) 385, 448.
- [35] P. Colangelo and A. Khodjamirian, hep-ph/0010175.
- [36] S. Narison and R. Tarrach, Phys. Lett. **125 B** (1983) 217.
- [37] T. Barnes, S. Godfrey and E. S. Swanson, Phys. Rev. **D72** (2005) 054026.
- [38] D. Becirevic, G. Duplancic, B. Klajn, B. Melic and F. Sanfilippo, Nucl. Phys. **B883** (2014) 306.
- [39] V. A. Novikov, L. B. Okun, M. A. Shifman, A. I. Vainshtein, M. B. Voloshin and V. I. Zakharov, Phys. Rept. **41** (1978) 1.
- [40] P. Ball and R. Zwicky, Phys. Rev. **D71** (2005) 014029.
- [41] P. Ball and V. M. Braun, Phys. Rev. **D54** (1996) 2182.
- [42] K. C. Yang, Nucl. Phys. **B776** (2007) 187.
- [43] Z. G. Wang, Eur. Phys. J. **C75** (2015) 427.
- [44] A. Khodjamirian and R. Ruckl, Adv. Ser. Direct. High Energy Phys. **15** (1998) 345.
- [45] Z. G. Wang, Eur. Phys. J. **C76** (2016) 387.